Rational Design of Dibenzothiophene-Based Host Materials for PHOLEDs

ARTICLE *in* THE JOURNAL OF PHYSICAL CHEMISTRY C · JANUARY 2014

Impact Factor: 4.77 · DOI: 10.1021/jp412107g

7 AUTHORS, INCLUDING:

Lin-Song Cui
Kyushu University
29 PUBLICATIONS **227** CITATIONS
SEE PROFILE

Zuo-Quan Jiang
Soochow University (PRC)
60 PUBLICATIONS **856** CITATIONS
SEE PROFILE

L. S. Liao
Soochow University, Suzhou, China
188 PUBLICATIONS **3,260** CITATIONS
SEE PROFILE

THE JOURNAL OF PHYSICAL CHEMISTRY C

Article

pubs.acs.org/JPCC

Rational Design of Dibenzothiophene-Based Host Materials for PHOLEDs

Shou-Cheng Dong, Lei Zhang, Jian Liang, Lin-Song Cui, Qian Li, Zuo-Quan Jiang,* and Liang-Sheng Liao*

Jiangsu Key Laboratory for Carbon-Based Functional Materials & Devices, Institute of Functional Nano & Soft Materials (FUNSOM), Soochow University, Suzhou, Jiangsu 215123, P. R. China

Supporting Information

ABSTRACT: A series of systematical designed host materials based on dibenzothiophene (DBT) were synthesized. Their physical properties were comprehensively characterized and compared with classic carbazole analogues. The different electron donating abilities of DBT and carbazole play an important role in the structure−property correlations. In this report, we demonstrate that the charge transport balance of host materials can be manipulated by utilizing the less electron-donating nature of DBT with proper design. Both the experimental data and theoretical calculations indicated possible bipolar property in meta-linked materials based on DBT. Through single carrier devices, an atypical bipolar transporting property was found in *m*-TPDBT. The meta- and ortho-linked DBT based materials exhibit decent performance in FIrpic based PHOLEDs. The best performed *m*-TPDBT was used as host in white phosphorescent organic light emitting diodes (PHOLEDs). Promising results were achieved with both double and single emitting layer configurations. A maximum power efficiency of 41.0 lm W^{-1} was achieved for warm white devices.

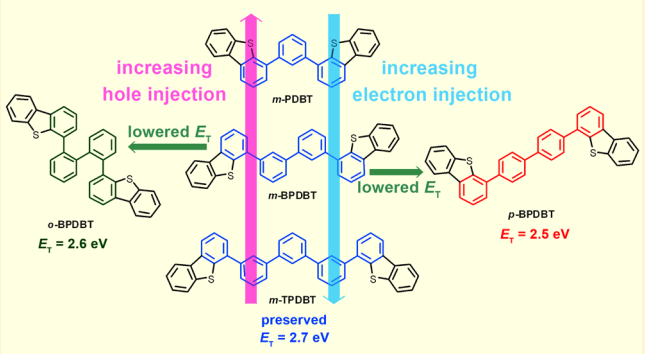

INTRODUCTION

Since the invention of the first practical organic light emitting diode (OLED),[1] it has drawn lots of attention from both academia and industry. Great efforts have been devoted to the development of OLED technology. Portable devices utilizing OLED display panels have already been competing front-to-front with high performance LCDs. From the first generation fluorescent device to the highly efficient phosphorescent device[2−4] and, very recently, the cutting edge hyperfluorescent device,[5−7] OLEDs have been gradually perfected over two decades. In all these milestones for OLEDs, the most efficient device structures contain a doped emitting layer (EML), which consisted of a host and a dopant. The high-in-energy host transfers the excitons generated by the injected carriers to the highly efficient dopant, resulting in an emission from the dopant. Generally, a good host material demands certain criteria. First, the energy of the host should be higher than the dopant, either S_1 or T_1 depending on the type of the dopant. Then, as the major component of the EML, matching HOMO/LUMO levels with adjacent layer, and balanced mobility are essential to the efficient carrier injection and recombination.[8] In addition, the host materials should also have good thermal stability. As the most promising and currently the most efficient OLED, phosphorescent OLEDs (PHOLEDs) have received extensive study.[8−10] Besides those criteria for host materials in general, a T_1 higher than 2.6 eV is preferred for host materials used in blue and white PHOLEDs, since the T_1 of typical sky blue triplet emitter is ca. 2.6 eV.[9] From the classic hole transporting host, i.e. *m*CP and CBP, to more advanced bipolar hosts,[11−15] carbazole is always an important constructing unit in the design of host. Its electron-donating nature ensures the hole injection and endows the materials with decent hole mobility. Carbazole also has a high T_1 of 3.0 eV, leaving abundant structural modification possibilities. But the lack of electron transporting property in carbazole usually requires the attachment of electron withdrawing group (EWG) to balance the carrier transport.[11−15] Is it possible to achieve bipolar property without introducing any EWG? In fluorescent materials, MADN and rubrene, which have no EWG, exhibit bipolar transporting property in OLED devices.[16−21] MADN can be used as a common material for hole transport, host of emitting, electron transport in the same device.[22] Compared to carbazole, they are more neutral molecules in structure. Their highly conjugated structure allows the delocalization of both injected electrons and holes. However, the low triplet energies impede their application as host materials in blue PHOLEDs. Recently, another heterocyclic unit similar to carbazole, dibenzothiophene (DBT), was utilized in constructing new

Received: December 10, 2013
Revised: January 14, 2014
Published: January 15, 2014

   dx.doi.org/10.1021/jp412107g | *J. Phys. Chem. C* 2014, 118, 2375−2384

Scheme 1. DBT-Based Host Materials

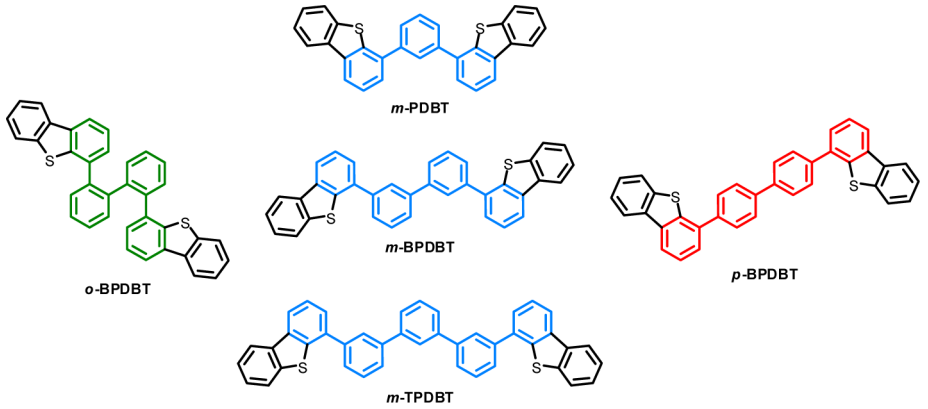

host materials.[23−28] It also possesses high T_1, like carbazole, but less electron-donating ability. The bromination of carbazole ring can proceed in mild conditions like NBS in $CHCl_3$ within hours. While DBT needs a fiercer reagent like Br_2 to proceed with the reaction and prolonged reaction time, which make DBT chemically a more inert, or neutral, unit than carbazole. Among those reported DBT containing host materials, many of them exhibit low-lying LUMO levels, comparable to some electron transporting materials.[23,25,28] In our previous work, DBT unit was incorporated with different spiro-structures.[29,30] The resulting materials exhibited very good device performances, and low-lying LUMOs were also observed, indicating that the presence of the DBT group will lower the LUMO of the host. The matching LUMO with electron transporting layer may facilitate the electron injection and enhance electron transport in the emitting layer. Adachi reported a DBT substituted triphenylene with bipolar property as host materials for red PHOLEDs,[31] and this material also possesses a low-lying LUMO. Very recently, a carbazole/DBT hybrid material was reported with bipolar transporting property, where the DBT unit was proposed as the electron-transporting channel.[32] These reported results suggest a possible electron transporting property of DBT group in OLED devices. On the other hand, the DBT segment was widely used in OFET materials exhibiting high hole mobility[33−36] due to its p-type nature. So, is it possible to construct bipolar host materials just using DBT group? Bearing this idea in mind, we designed a series of DBT based materials using phenyl spacer to link two DBT moieties (Scheme 1), following the classic configurations for carbazole-based hosts. Comprehensive characterizations have been done to understand the correlation between molecular structure configuration and physical properties. An atypical bipolar property of a DBT-based host material was revealed. Blue and white PHOLEDs were also fabricated using these materials, demonstrating their ability as efficient host materials for PHOLEDs.

RESULTS AND DISCUSSION

Synthesis and Characterization. Scheme 2 illustrates the synthetic route of the host materials. The synthesis is straightforward with classic Suzuki−Miyaura reaction. The yield of each step was very high (above 80%). The final products were characterized by ^{1}H NMR and ^{13}C NMR spectroscopies, mass spectrometry, and elemental analysis. All the materials have good solubility in common organic solvents (CH_2Cl_2, $CHCl_3$, THF, etc.) except *p*-BPDBT. Its linear rigid

Scheme 2. Syntheses of Materials

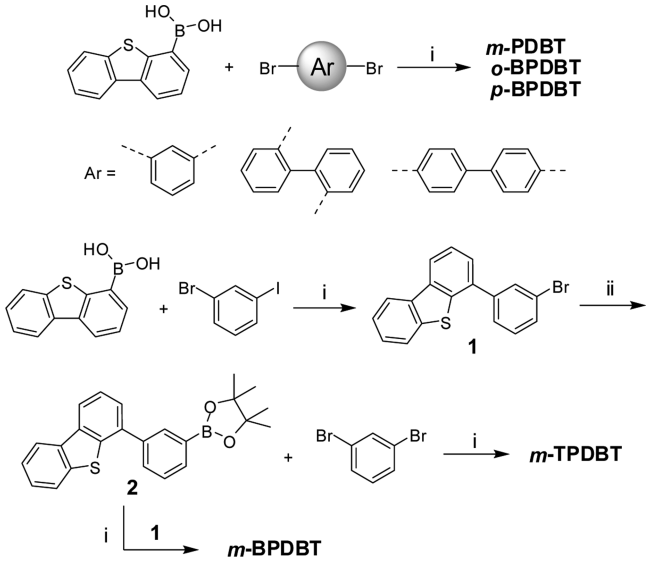

structure makes it hardly soluble in common solvents. All the materials were further purified by vacuum sublimation before device fabrication.

Thermal Analysis. The thermal stabilities of the materials were characterized by thermogravimetric analysis (TGA). All the materials show T_d over 300 °C (Figure S1). *m*-TPDBT has the highest T_d of 390 °C. Glass transition temperatures (T_g) were obtained using differential scanning calorimetry (DSC). The meta-linked materials exhibit gradually increased T_g from 79 to 102 °C as the spacers between DBT units extended (Figure 1), similar to what was observed in carbazole analogues (vide infra). No obvious glass transition process was observed for *o*-BPDBT and *p*-BPDBT.

Photophysical Properties. Figure 2 illustrates the UV−vis absorption and photoluminescence (PL) spectra in dilute CH_2Cl_2 solutions at room temperature and phosphorescent spectra in 2-methyltetrahydrofuran at 77 K. The relatively weak shoulder peaks at ca. 330 nm which appeared in absorption spectra of all these materials can be attributed to the n−π^* transitions of the DBT group. Meta-linked materials show similar absorption spectra and almost identical PL and phosphorescent spectra due to their restrained conjugation length by meta-linkage. As a merit of meta-linkage, the extended phenyl spacers did not affect their photophysical properties. All these materials exhibit structureless, broad

dx.doi.org/10.1021/jp412107g | J. Phys. Chem. C 2014, 118, 2375−2384

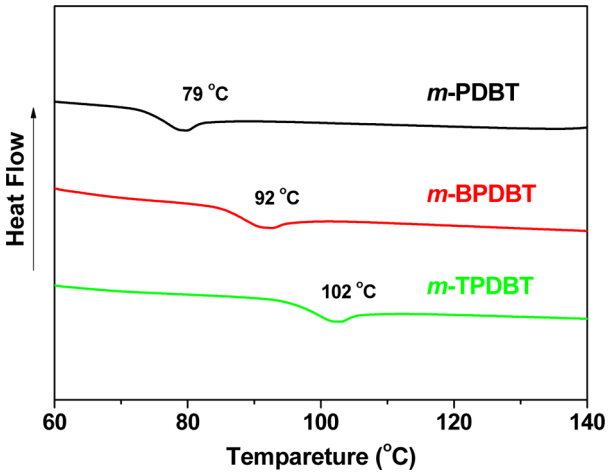

Figure 1. DSC traces recorded at a heating rate of 10 °C min^{-1}.

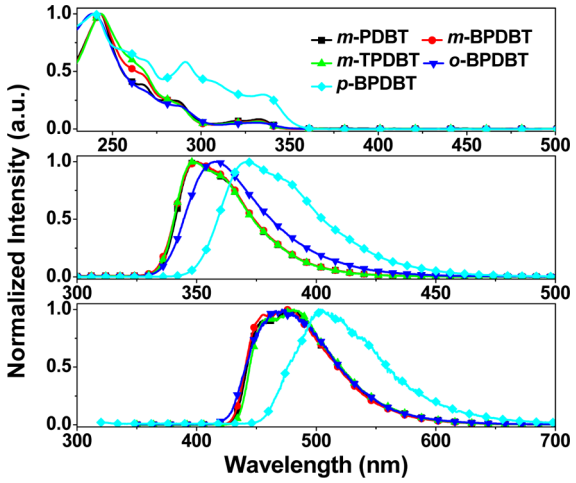

Figure 2. UV−vis absorption and PL spectra measured in CH_2Cl_2 solution at 10^{-5} M; phosphorescence spectra measured in frozen 2-methyltetrahydrofuran (2-MeTHF) matrix at 77 K.

phosphorescent spectra. The triplet energies of *m*-PDBT, *m*-BPDBT, and *m*-TPDBT are all above 2.7 eV, sufficient enough to be used as blue host for sky blue triplet emitters. Ortho-linked *o*-BPDBT shows slightly narrowed bandgap and red-shifted PL spectrum. Its triplet energy is slightly lower than meta-linked ones (2.64 eV). The influence of increased effective conjugation length on the E_T of *o*-BPDBT is partially compensated by the steric hindrance caused by its distorted configuration, preserving the E_T. As expected, *p*-BPDBT shows significantly red-shifted PL spectrum and lowered E_T (2.46 eV) due to its linear structure with profoundly increased effective conjugation length. In order to get the bandgap of these materials in solid state, UV−vis absorption spectra of vacuum-deposited thin films were measured (Figure S2). Meta- and ortho-linked materials show similar absorption spectra as to their solution with only slightly narrowed bandgap. While due to the rigid linear configuration of *p*-BPDBT, its absorption spectrum shows a pronounced red-shift and its optical bandgap narrows by 0.2 eV. All the physical data of these materials are summarized in Table 1.

Electrochemical Properties and FMO Energy Levels. The electrochemical behaviors of these materials were measured using a typical trielectrode configuration with ferrocene as internal standard. All the materials show distinct oxidation processes (Figure 3) corresponding to the oxidation

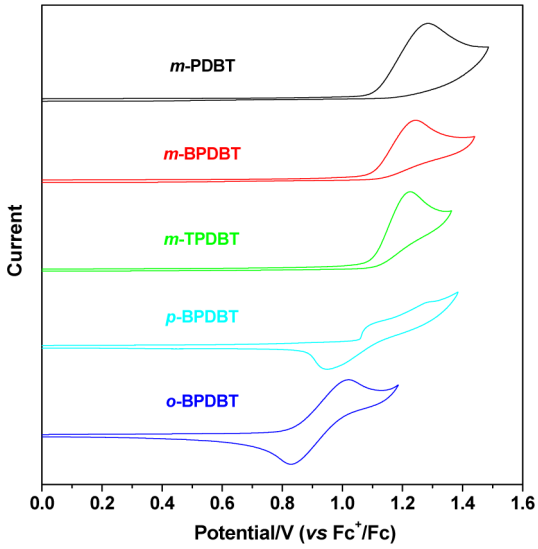

Figure 3. Cyclic voltammogram of host materials. The measurements were performed in CH_2Cl_2 with 0.1 M of *n*-Bu_4NPF_6 as supporting electrolyte.

of the sulfur atom. Nevertheless, no obvious reduction processes were observed. Meta-linked materials exhibited an irreversible oxidation peak, while *o*-BPDBT and *p*-BPDBT show reversible oxidation processes. This difference is probably caused by the more conjugated configuration of ortho- and para-linkage delocalizing and stabilizing the oxidized state. In order to get more accurate energy levels, HOMOs of solid thin films were determined by ultraviolet photoemission spectroscopy (UPS) technique (Figures S4−S8). LUMO levels were

Table 1. Physical Properties

	abs λ_{max} solution[a]/film[b] [nm]	PL λ_{max} solution[a]/film[b] [nm]	E_T[c] [eV]	T_m[d] [°C]	T_g[d] [°C]	T_d[d] [°C]	HOMO[e] [eV]	LUMO[f] [eV]	E_g[g] solution [eV]	E_g[g] film [eV]
m-PDBT	333, 285, 267/337, 289	350/370	2.73	191	79	303	6.21	2.69	3.60	3.52
m-BPDBT	333, 287, 266/336, 288	350/368	2.72	186	92	339	6.19	2.65	3.60	3.54
m-TPDBT	332, 285, 265/337, 289	349/364	2.71	>300	102	390	6.30	2.80	3.61	3.50
o-BPDBT	332, 289, 268/338, 291	358/365	2.64	281		304	6.17	2.69	3.54	3.48
p-BPDBT	336, 291, 267/343, 319, 297	371/393, 413, 436	2.46	270		358	6.10	2.78	3.51	3.32

[a]Measured in diluted CH_2Cl_2 solution at room temperature. [b]Vacuum-deposited thin film (40 nm). [c]Measured in 2-MeTHF glass matrix at 77 K. [d]T_m: melting temperatures; T_g: glass transition temperatures; T_d: decomposition temperatures. [e]HOMO levels were calculated from UPS data. [f]LUMO levels were calculated from HOMO and E_g in solid films. [g]E_g: the band gap energies were calculated from the corresponding absorption onset.

dx.doi.org/10.1021/jp412107g | J. Phys. Chem. C 2014, 118, 2375−2384

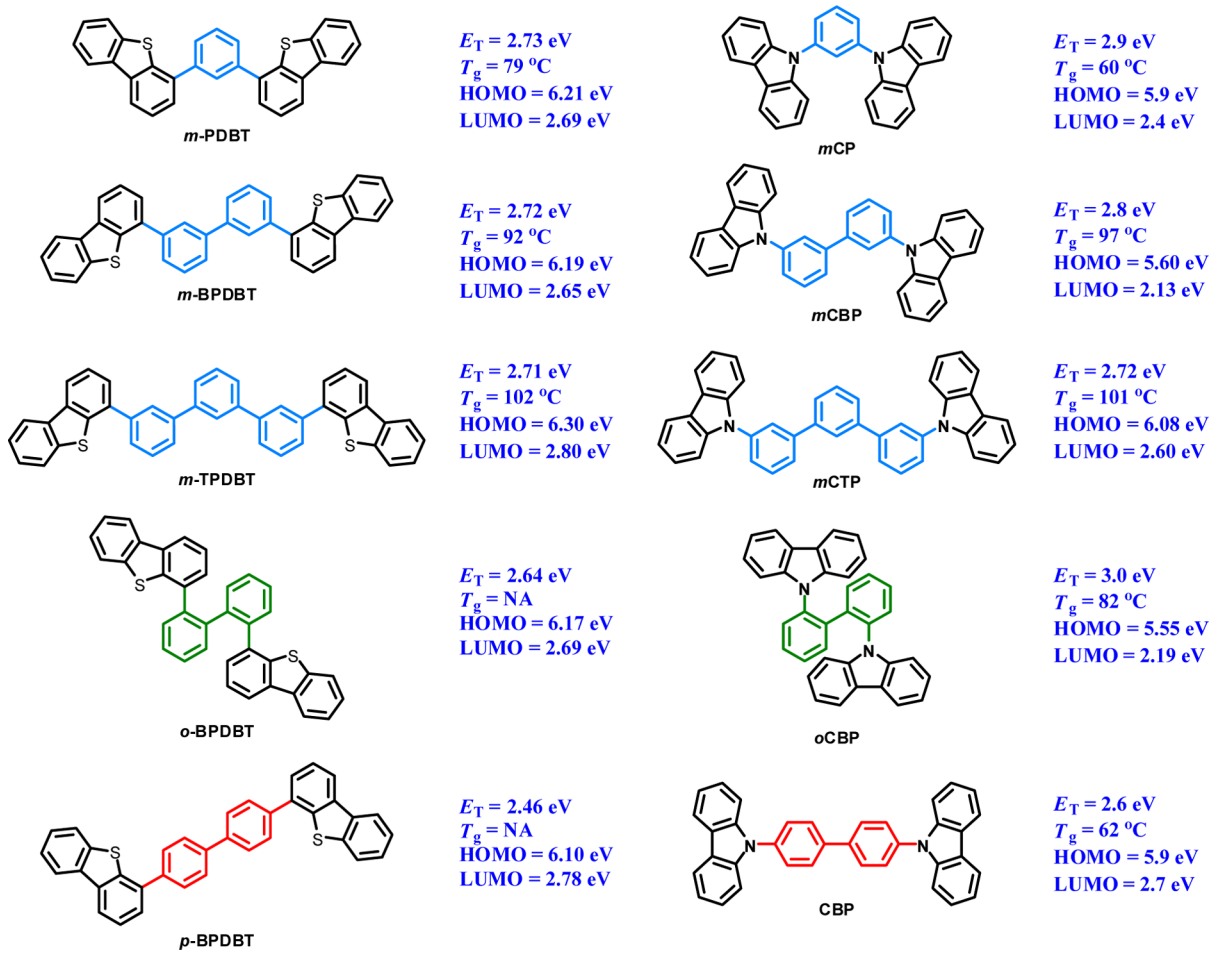

Figure 4. Summary of physical properties for DBT and carbazole derivatives.

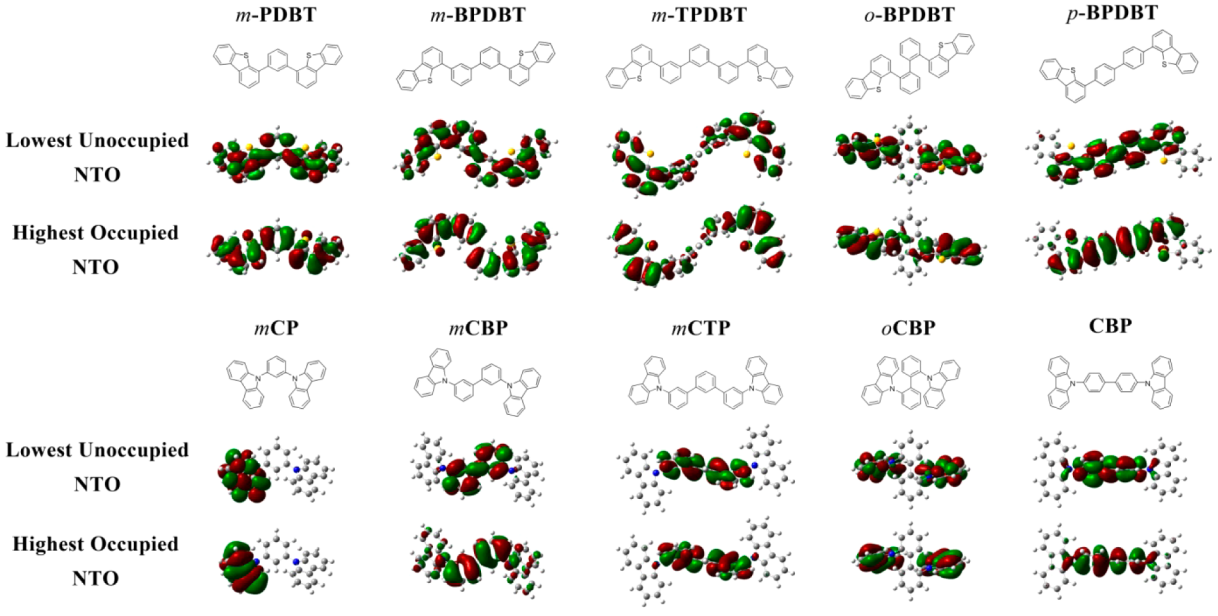

Figure 5. Natural transition orbitals of DBT and carbazole derivatives.

calculated by HOMO and the optical bandgap of deposited films. All these materials exhibit relatively low HOMO and LUMO compare to traditional carbazole host materials. The lowered FMO energies reflect the different electronic structures of these materials and affect their device performances. The detailed discussion will be elaborated in the following sections.

Comparison of DBT and Carbazole Analogues. Carbazole derivatives have been extensively explored as host

dx.doi.org/10.1021/jp412107g | J. Phys. Chem. C 2014, 118, 2375−2384

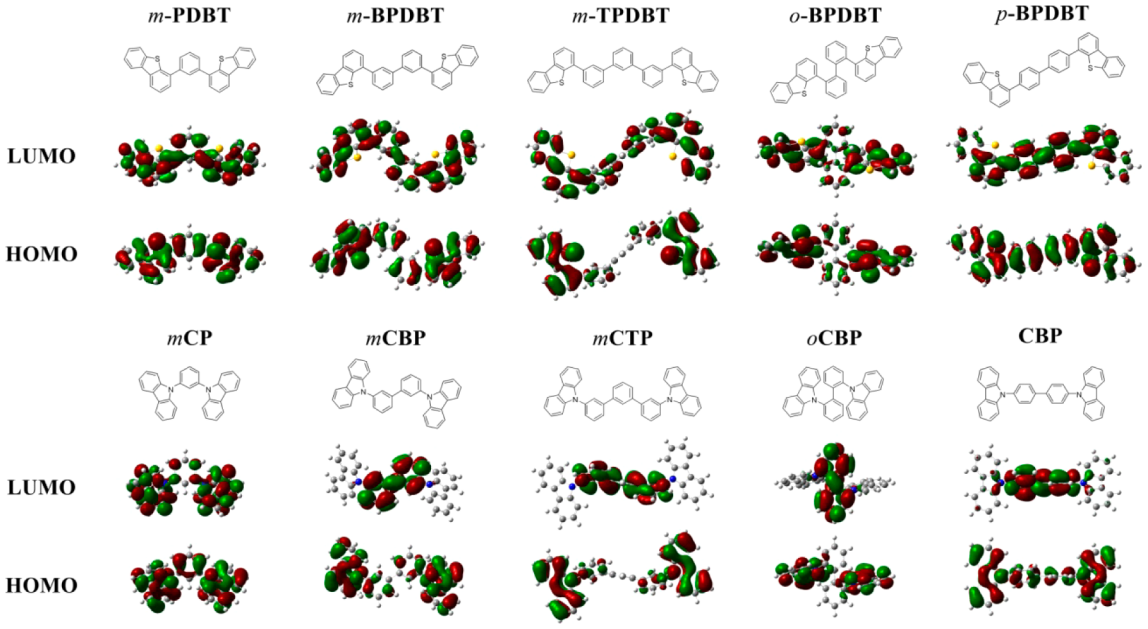

Figure 6. Optimized geometry and HOMO−LUMO spatial distributions.

materials over decades. Our design strategy follows the footprint of the development of phenyl carbazole derivatives. For each DBT-based material in this report, there is a carbazole counterpart bearing similar molecular configuration with well-established properties.[9,37,38] Figure 4 shows the structures and some key physical properties of DBT- and carbazole-based materials. Meta-linked materials show very similar thermal property trending. With extended phenyl spacers, the T_g gradually increases from below 80 °C to above 100 °C, indicating that the different linking position on DBT and carbazole did not affect the thermal property. The T_gs are mainly determined by the phenyl spacer and the molecular weight. *o*-BPDBT and *p*-BPDBT did not exhibit obvious glass transition process on their DSC traces due to their tendency to crystallize, indicating potentially low T_g, similar to their carbazole counterparts, *o*CBP and CBP.

Another critical physical property for a host material is the triplet energy, which directly determines their ability as host for triplet emitters, especially important for blue and white PHOLEDs. CBP, which has an E_T of 2.6 eV, showed significantly lowered efficiency than *m*CP (E_T = 2.9 eV) in sky blue PHOLEDs due to the inefficient energy transfer from host to dopant. Meta-linkage is a popular and effective way to maintain high triplet energy while still expands the π-conjugation system. From the experiment data reported in the literature, the meta-linked *m*CP, *m*CBP, and *m*CTP exhibit gradually declined E_T, from 2.9 to 2.7 eV. In our DBT system, all three meta-linked molecules show similar E_T around 2.7 eV. Time-dependent DFT calculation was utilized to further investigate the triplet states of these materials. Their natural transition orbitals (NTO)[39] defining the T_1 states are depicted in Figure 5. DBT-based materials show very different wave functions compared to their carbazole counterparts. The NTOs of *m*-PDBT and *m*-BPDBT are delocalized over the entire molecules. As the phenyl spacer continues to extend, the NTO of *m*-TPDBT is mainly localized on the phenyl-4-DBT moieties at each side. This phenomenon indicates that the T_1 states of meta-linked DBT materials are characterized by the transition localized on phenyl-4-DBT group, which explains the nearly unchanged E_T of the meta-linked DBT materials. On the contrary, the NTO of *m*CP distribute entirely on the carbazole ring, resulting in a high E_T of 2.9 eV. While with the extension of the phenyl spacer, the NTO gradually shifted to the benzene rings, showing gradually declined triplet energies. As for ortho-linked structures, *o*CBP shows more distorted configuration than *o*-BPDBT due to the different linking position, thus resulting in higher E_T. Para-linked *p*-BPDBT and CBP have similar low E_T due to the extended conjugation length. *p*-BPDBT shows lower E_T than CBP because of the highly conjugated *p*-quaterphenyl unit in its structure, which defines its T_1 state.

For host materials, appropriate HOMO and LUMO energy levels are essential to the efficient injection of carriers into the emitting layer. The HOMO and LUMO of carbazole- and DBT-based hosts are listed in Figure 4 for comparison. The values of the HOMOs and LUMOs of *m*CBP and *o*CBP were obtained from CV data;[38] however, HOMOs and LUMOs of the other materials were determined by UPS. Compared to CV results, HOMOs obtained from UPS spectra of solid thin films are more reliable. We also tested the UPS spectrum of *m*CBP (Figure S9) which shows a HOMO of 6.0 eV. According to the experiential correlation between the HOMO value obtained by UPS and CV method[40,41] and the theoretical results, it is reasonable to correct the HOMO of *o*CBP to ca. 6.0 eV, similar to *m*CBP. Since the LUMO are calculated using HOMO and E_g, the LUMO of *m*CBP and *o*CBP also can be adjusted to ca. 2.5 eV. Basically, these carbazole derivatives show HOMOs of ca. 6.0 eV and LUMOs varying from 2.4 to 2.7 eV depending on the effective conjugation length. Meanwhile, the DBT-based materials show significantly lowered energy levels with HOMOs of 6.1−6.3 eV and LUMOs of 2.7−2.8 eV. The different physical properties of DBT and carbazole determine their different energy levels. The central amine in carbazole is a stronger electron donor than the sulfur in DBT. As a result, the DBT moiety is more difficult to be oxidized than carbazole. The oxidation potential of *m*CBP is about 0.3 eV smaller than *m*-BPDBT,[38] matching with the UPS results. Thus, the DBT-based materials show much lower HOMO. Meanwhile, the

dx.doi.org/10.1021/jp412107g | J. Phys. Chem. C 2014, 118, 2375−2384

bandgaps of DBT and carbazole are basically the same because of the similar contributions of the central amine and sulfur to the HOMO and LUMO.[42] Moreover, these DBT materials have the same linking strategies to their corresponding carbazole analogues. As a result, the bandgaps of these DBT materials are very close to their carbazole counterparts, leading to lower LUMO.

To better understand the different FMO of these DBT- and carbazole-based materials, DFT calculations were carried out to simulate their HOMO and LUMO (Figure 6). These materials exhibit very similar HOMO to their corresponding carbazole analogues. In meta- and ortho-linked molecules, the HOMO mainly locates on the carbazole and DBT moieties, due to the restrained effective conjugation length, with minor occupation on the adjacent benzene ring. The heavy populations on the amine and sulfur units suggest their electron-donating nature. Interestingly, these materials show very different LUMO distributions compared with their carbazole equivalents. *m*CP exhibits LUMO on the whole molecule similar to its HOMO. In all the other carbazole derivatives, the LUMOs mainly localize on the central phenyl spacer due to the large torsion angle between the nitrogen donor on carbazole and the phenyl spacer. While for those DBT-based materials, the LUMOs delocalize over the entire molecule, regardless of the linking strategies and the spacer length. The significant MO interactions between phenyl spacers and benzene rings in DBT units extend the LUMO to the whole system, bypassing the S atom. The less electron-donating property of the sulfur atom readily decreases the LUMO of the DBT moiety and the phenyl spacer. Hence, the DBT-based materials exhibit substantially lowered HOMOs and LUMOs. To assess the FMO distributions quantitatively, the HOMO and LUMO wave functions of these materials were decomposed to atomic level (using Hirshfeld partition by percentage)[43] and then summed up according to functional structure moieties, and the results are shown in Figure 7. It is clear that the HOMO

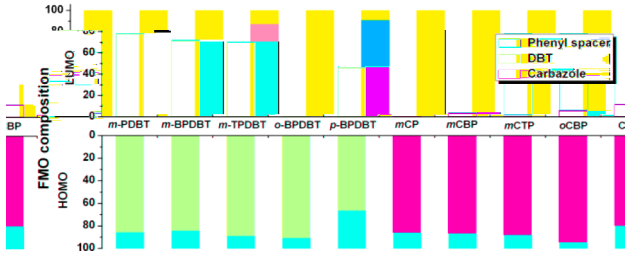

Figure 7. FMO compositions by different moieties. Orbital composition analysis was performed using Multiwfn.[43]

compositions of these materials are very similar. Both DBT and carbazole take up over 80% population, except the highly conjugated *p*-BPDBT. In the LUMO compositions, *m*CP aside, the carbazole derivatives have less than 13% population on carbazole ring. *m*CBP and *m*CTP only show very low distributions of 3.9% and 2.0%, respectively. On the other hand, DBT-based materials have a large proportion of LUMO on the DBT group. In *m*-BPDBT and *m*-TPDBT, the DBT units take up 71.8% and 70.0% of the LUMO. Considering there are two DBT units in each molecule, the two DBT units and the phenyl spacer each take up approximately one-third of the LUMO, which further confirm that the LUMO of these two materials are distribute evenly throughout each of the structures. Unlike carbazole derivatives, which the electrons will be injected on the phenyl spacers, DBT materials may stabilize the injected electrons with its delocalized and evenly distributed LUMO wave functions, making these materials more tolerable to negative charges. The replacement of carbazole with DBT group significantly lowers the HOMO and LUMO energies, possibly facilitating electron injection, and combined with the p-type nature of DBT moiety, the meta-linked DBT materials with evenly distributed LUMO may possibly exhibit some kind of bipolar transporting property in OLED devices.

Therefore, to evaluate their charge carrier transporting ability, hole-only and electron-only devices were fabricated using following structures: ITO/MoO_3 (5 nm)/Host (100 nm)/MoO_3 (5 nm)/Al (hole); ITO/TmPyPB (20 nm)/Host (100 nm)/Liq (2 nm)/Al (electron). Most of these DBT-based materials show predominated hole transporting properties. Interestingly, as the phenyl spacers become longer, the current densities of meta-linked materials decrease in hole-only devices but increase in electron-only devices (Figure S10). Lastly, as expected, crossed $J-V$ curves for holes and electrons were observed in *m*-TPDBT-based devices (Figure 8), indicating a

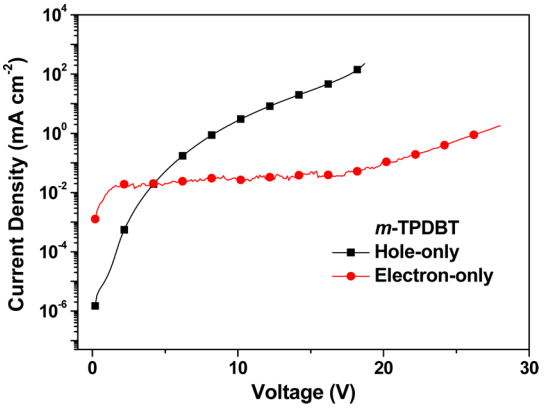

Figure 8. $J-V$ curves of hole-only and electron-only devices.

bipolar transporting property. When the driving voltage is below 4.3 V, the current density for electron-only device is much higher than that of hole-only device. As the voltage increases, the current density for holes climbs rapidly, while the current density for electron shows much slower increase. At about 10 V, the current density for holes is already 2 magnitudes higher than that of electrons. At ca. 4.3 V, this material shows comparable hole and electron transporting abilities. The possible cause of this atypical bipolar property is that the low-lying and evenly distributed LUMO, which facilitates the electron injection and provides this material relatively high electron mobility at low voltage. As the driving voltage increase, the electron-donating nature of DBT moiety starts to take effect, resulting a rapid climb of hole mobility. Within the typical operating voltage for PHOLEDs (ca. 3.0−6.0 V), *m*-TPDBT shows bipolar transporting property, which may improve its device performance.

EL Performance of PHOLEDs. Considering the triplet energy levels, *p*-BPDBT is not suitable for blue host material. Only meta- and ortho-linked materials were used as host materials for FIrpic-based devices. A device configuration of ITO/*m*CP:MoO_3 15 wt % (45 nm)/*m*CP (10 nm)/Host:8 wt % FIrpic (20 nm)/TmPyPB (40 nm)/Liq (2 nm)/Al was adopted to evaluate the performance of these four materials.

dx.doi.org/10.1021/jp412107g | J. Phys. Chem. C 2014, 118, 2375−2384

MoO_3-doped *m*CP was used as hole injection layer (HIL) and hole transport layer (HTL) followed by another thin layer of *m*CP functioning as electron blocking layer (EBL). *m*-PDBT (B1), *m*-BPDBT (B2), *m*-TPDBT (B3), or *o*-BPDBT (B4) were doped with 8 wt % FIrpic to form emitting layer (EML). TmPyPB which has high E_T and carrier mobility served as electron transporting/hole blocking layer (ETL/HBL) to confine triplet excitons in the EML. And Liq was utilized as electron injection layers (EIL). Figure 9 shows the performance

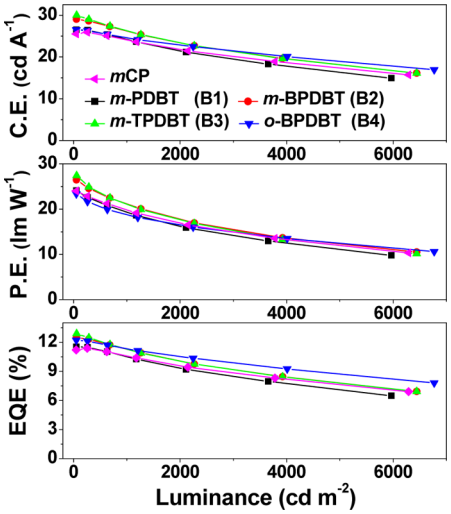

Figure 9. Device performances of devices B1−B4 and control device (*m*CP).

of blue OLED devices. All four materials exhibit comparable or superior efficiencies than control device using *m*CP as host materials. Meta-linked materials show increased efficiencies as the phenyl spacer extends. *m*-TPDBT has the highest efficiencies with maximum current efficiency (CE) of 30.0 cd A^{-1}, power efficiency of 27.4 lm W^{-1}, and external quantum efficiency (EQE) of 12.9%. All these devices show low roll-off with less than 15% drop for EQEs at 1000 cd m^{-2} compared to their maximum values. Although the E_T of *o*-BPDBT is not very high (2.64 eV), it still achieved pretty decent performance with a maximum EQE of 12.2% and a low roll-off of 7% at 1000 cd m^{-2}. Detailed performance data are summarized in Table 2.

Then warm white PHOLEDs were fabricated using the best performed *m*-TPDBT. Adopting PO-01 as yellow dopant, double emitting layer PHOLEDs were constructed by simply replacing the emitting layer of blue devices with (*m*-TPDBT:3 wt % PO-01 (*x* nm)/*m*-TPDBT:8 wt % FIrpic (10-*x* nm), *x* is 0.5 for W1, 1.0 for W2, and 2.0 for W3). Surprisingly, these PHOLEDs exhibit very unstable spectra (Figure 10c). The CIEs of W1−W3 shift from yellow white to greenish-blue (Figure S15). These severe color changes are obviously caused by the shift of the charge recombination zones. The decreasing slopes (Figure 10e) of CIE coordinates are very close regardless to the thickness of PO-01 layer, indicating a similar recombination zone shifting length in W1−W3 related to the host material. Figure 11 shows the proposed energy diagram for PHOLEDs. The low-lying LUMO (2.8 eV) of *m*-TPDBT perfectly matches with ETL. There is no injection barrier at the EML/ETL interface. But at the hole injection side, the deep HOMO of *m*-TPDBT create an injection barrier of 0.4 eV. Moreover, PO-01, which has a high-lying HOMO of 5.1 eV, can act like hole trapping sites in the yellow EML. So, from the perspective of energy levels, the recombination zone will locate at the EBL/EML interface. As discussed in the last section, the *m*-TPDBT exhibits electron transporting property at low driving voltages, making it an electron-transporting host material. As a result, the recombination zone indeed locates at the EBL/EML interface at low current densities. W1−W3 exhibit yellowish-white to greenish-white emission at 0.2 mA cm^{-2}, depending on the thickness of yellow EML. As the current density increases, the hole mobility of *m*-TPDBT climbs rapidly, turning it into a hole-transporting material. The injection barrier at the EBL/EML interface can be overcome upon increased driving voltage. Thus, the recombination zone gradually moves toward the cathode with increasing current density, resulting successively blue-shifting CIE coordinates. This phenomenon verified our discovery in the single carrier devices. Color shifts aside, W1−W3 exhibit moderate efficiencies. With the increase of yellow EML, the devices show a small growth in current and power efficiencies but slight decline in EQE due to the yellow-shifted CIEs. W3 has a maximum efficiency of 39.0 cd A^{-1}, 31.3 lm W^{-1}, and 11.5%. The results of W1−W3 indicate this double EML structure is not suitable for this material in purpose of white light emitting. But the unique property of this host suggests its potential in color-tunable OLEDs in some special applications. Most of those color tunable devices request delicate design and relatively complicate structures.[44,45] With the reversible transporting property of *m*-TPDBT, the device structure can be

Table 2. Electroluminescence Characteristics of the Devices

device[a]	host	V^b [V]	$\eta_{ce}{}^c$ [cd A^{-1}]	$\eta_{pe}{}^c$ [lm W^{-1}]	$\eta_{ext}{}^c$ [%]	CIE[d] [*x*, *y*]
B1	*m*-PDBT	3.9	26.5, 26.5, 24.1	24.1, 23.8, 19.4	11.5, 11.5, 10.5	0.15, 0.36
B2	*m*-BPDBT	3.9	29.0, 28.9, 26.2	26.5, 26.1, 21.0	12.5, 12.4, 11.3	0.15, 0.37
B3	*m*-TPDBT	3.9	30.0, 29.8, 26.3	27.4, 27.1, 21.1	12.9, 12.8, 11.2	0.15, 0.37
B4	*o*-BPDBT	4.1	26.5, 26.5, 24.7	23.4, 23.1, 18.8	12.2, 12.2, 11.3	0.14, 0.33
W1		4.7	34.5, 34.2, 29.8	28.4, 27.8, 20.1	12.0, 12.0, 11.3	0.23, 0.41
W2		4.7	37.5, 37.2, 32.0	30.4, 29.9, 21.5	11.7, 11.7, 10.9	0.31, 0.45
W3	*m*-TPDBT	4.7	39.0, 38.8, 33.2	31.3, 30.9, 21.4	11.5, 11.4, 10.3	0.40, 0.49
W4		3.9	41.0, 40.8, 36.0	37.3, 37.1, 29.3	14.1, 14.1, 12.8	0.29, 0.43
W5		3.9	45.0, 45.0, 42.6	41.0, 40.9, 34.3	13.3, 13.2, 12.7	0.42, 0.50

[a]Device configuration: B1−B4, ITO/*m*CP:MoO_3 15 wt % (45 nm)/*m*CP (10 nm)/Host:8 wt % FIrpic (20 nm)/TmPyPB (40 nm)/Liq (2 nm)/Al; W1−W3, ITO/*m*CP:MoO_3 15 wt % (45 nm)/*m*CP (10 nm)/*m*-TPDBT:3 wt % PO-01 (*x* nm)/*m*-TPDBT:8 wt % FIrpic (10-*x* nm)/ TmPyPB (40 nm)/Liq (2 nm)/Al, *x* = 0.5, 1.0, 2.0; W4/W5, ITO/*m*CP:MoO_3 15 wt % (45 nm)/*m*CP (10 nm)/*m*-TPDBT: 8 wt % FIrpic: *x* wt % PO-01 (20 nm)/TmPyPB (40 nm)/Liq (2 nm)/Al, W4/W5 *x* = 0.2/0.5. [b]Voltages at 1000 cd m^{-2}. [c]Efficiencies in the order of maximum, at 100 cd m^{-2} and at 1000 cd m^{-2}. [d]Commission International de I'Eclairage coordinates measured at 5 mA cm^{-2}.

dx.doi.org/10.1021/jp412107g | J. Phys. Chem. C 2014, 118, 2375−2384

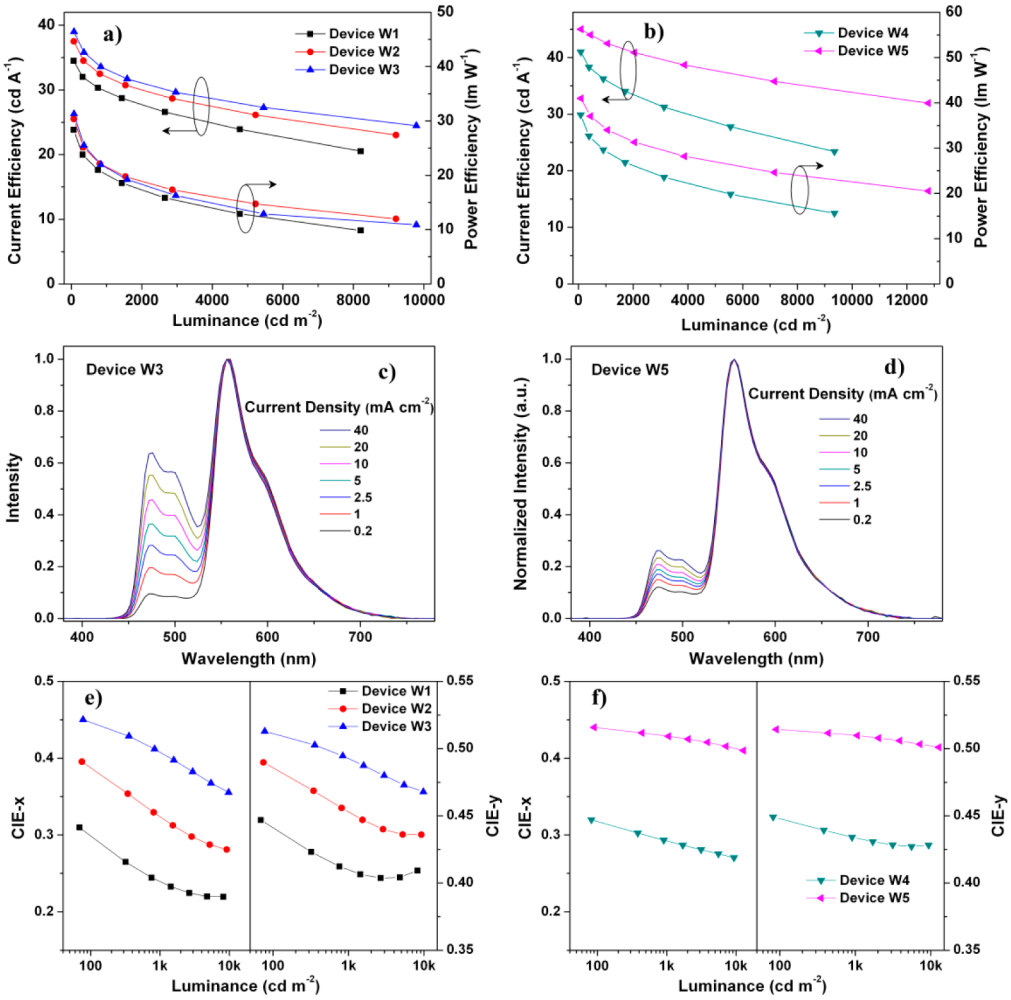

Figure 10. Current efficiencies and power efficiencies as a function of luminance for devices W1−W3.

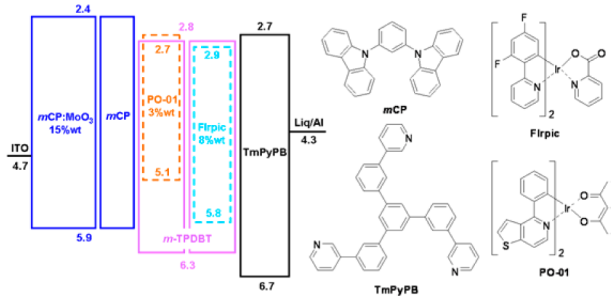

Figure 11. Proposed energy diagram of devices.

simplified. The color variation can be adjusted simply by choosing different dopant materials.

Although double EML PHOLEDs show unstable CIEs, there are still ways to stabilize the emitting spectra. Adding a buffer layer between two EMLs and merging the EMLs into one are two popular solutions to obtain stable CIE. Here we adopted the second option for the simplicity of the device. Single EML PHOLEDs were fabricated by doping FIrpic and PO-01 into one EML with different doping ratios (*m*-TPDBT: 8 wt % FIrpic: *x* wt % PO-01 (20 nm), *x* is 0.2 for W4 and 0.5 for W5). As expected, the EL spectra of W4 and W5 are much stable than W1−W3 (Figure 10d,f). The minor vibrations in EL spectra are probably caused by the microcavity effect induced by the recombination zone shifts.[46−48] The single EML configuration also reduces the driving voltages. The voltages at 1000 cd m^{-2} for W4 and W5 are 1.2 V lower than W1−W3, even with doubled EML thickness. W4 and W5 show good performances with a maximum EQE of 14.1% and 13.3%, respectively (Figure 12). W5 has a yellow white emission with maximum CE of 45.0 cd A^{-1} and PE of 41.0 lm W^{-1}, and W5 also shows very low efficiency roll-offs. At 1000 cd m^{-2}, the CE, PE, and EQE maintain 94.7%, 83.7%, and 95.5% of their

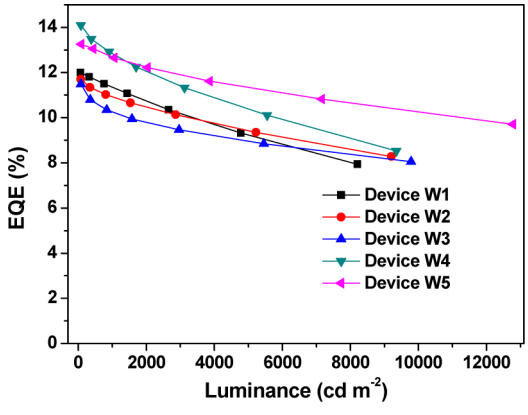

Figure 12. EQEs of white PHOLEDs W1−W5.

dx.doi.org/10.1021/jp412107g | J. Phys. Chem. C 2014, 118, 2375−2384

original values. The device performances verify the ability of these DBT-based materials as efficient host for PHOLEDs. Although the CIE of W5 is somewhat yellowish, the decent performance demonstrates the potential of *m*-TPDBT as an efficient host for white PHOLEDs. Moreover, the unique charge transporting property of *m*-TPDBT also opens up its application in color-tunable OLEDs.

CONCLUSION

Five dibenzothiophene-based host materials were designed and synthesized. Their design strategy followed the footprint of classic carbazole-based host materials with two dibenzothiophene groups connected by phenyl spacers with different configurations. The physical properties of these materials were comprehensively characterized and comparatively analyzed with corresponding to carbazole analogues. The dibenzothiophene-based materials exhibit dramatically different characteristics as results of the less electron-donating nature of dibenzothiophene compared to carbazole counterparts. The low-lying HOMO/LUMO levels and evenly distributed LUMO wave functions of meta-linked materials suggested possible electron transporting property. Along with the p-type nature of dibenzothiophene group, a bipolar transport property was predicted and found in *m*-TPDBT via single carrier devices. PHOLEDs were fabricated using meta- and ortho-linked materials. All the FIrpic-based devices exhibit good performance. The best-performed *m*-TPDBT was further evaluated in single and double emitting layer white PHOLEDs. In single emitting layer white devices, a maximum power efficiency of 41.0 lm W^{-1} was achieved. In this research, it is demonstrated that by proper design the charge transport property and other physical characteristics can be fine-tuned in these DBT-based host materials, revealing the potentials of dibenzothiophene as functional group in constructing bipolar host materials.

ASSOCIATED CONTENT

Supporting Information

Details of organic synthesis, characterization procedures of materials, theoretic calculation methods, and device performance features. This material is available free of charge via the Internet at http://pubs.acs.org.

AUTHOR INFORMATION

Corresponding Authors

*E-mail zqjiang@suda.edu.cn (Z.-Q.J.).
*E-mail lsliao@suda.edu.cn (L.-S.L.).

Notes

The authors declare no competing financial interest.

ACKNOWLEDGMENTS

We are grateful to the assistance of Dr. Cheng Zhong from Wuhan University in the DFT calculations. We acknowledge the financial support from the National Postdoctoral Science Foundation of China (no. 2012M511797), the Natural Science Foundation of China (no. 21202114, 21161160446, 61036009, and 61177016), the National High-Tech Research Development Program (no. 2011AA03A110), and the Natural Science Foundation of Jiangsu Province (no. BK2010003). This is also a project funded by the Priority Academic Program Development of Jiangsu Higher Education Institutions (PAPD) and by the Research Supporting Program of Suzhou Industrial Park.

REFERENCES

(1) Tang, C. W.; VanSlyke, S. A. Organic Electroluminescent Diodes. *Appl. Phys. Lett.* **1987**, *51*, 913−915.
(2) Baldo, M. A.; Lamansky, S.; Burrows, P. E.; Thompson, M. E.; Forrest, S. R. Very High-Efficiency Green Organic Light-Emitting Devices Based on Electrophosphorescence. *Appl. Phys. Lett.* **1999**, *75*, 4−6.
(3) Adachi, C.; Baldo, M. A.; Forrest, S. R.; Thompson, M. E. High-Efficiency Organic Electrophosphorescent Devices with Tris(2-phenylpyridine)iridium Doped into Electron-Transporting Materials. *Appl. Phys. Lett.* **2000**, *77*, 904−906.
(4) Baldo, M. A.; O'Brien, D. F.; You, Y.; Shoustikov, A.; Sibley, S.; Thompson, M. E.; Forrest, S. R. Highly Efficient Phosphorescent Emission from Organic Electroluminescent Devices. *Nature* **1998**, *395*, 151−154.
(5) Endo, A.; Sato, K.; Yoshimura, K.; Kai, T.; Kawada, A.; Miyazaki, H.; Adachi, C. Efficient Up-conversion of Triplet Excitons into a Singlet State and its Application for Organic Light Emitting Diodes. *Appl. Phys. Lett.* **2011**, *98*, 083302−1−083302−3.
(6) Zhang, Q.; Li, J.; Shizu, K.; Huang, S.; Hirata, S.; Miyazaki, H.; Adachi, C. Design of Efficient Thermally Activated Delayed Fluorescence Materials for Pure Blue Organic Light Emitting Diodes. *J. Am. Chem. Soc.* **2012**, *134*, 14706−14709.
(7) Uoyama, H.; Goushi, K.; Shizu, K.; Nomura, H.; Adachi, C. Highly Efficient Organic Light-Emitting Diodes from Delayed Fluorescence. *Nature* **2012**, *492*, 234−238.
(8) Wang, Q.; Ma, D. Management of Charges and Excitons for High-Performance White Organic Light-Emitting Diodes. *Chem. Soc. Rev.* **2010**, *39*, 2387−2398.
(9) Tao, Y.; Yang, C.; Qin, J. Organic Host Materials for Phosphorescent Organic Light-Emitting Diodes. *Chem. Soc. Rev.* **2011**, *40*, 2943−2970.
(10) Sasabe, H.; Kido, J. Multifunctional Materials in High-Performance OLEDs: Challenges for Solid-State Lighting. *Chem. Mater.* **2011**, *23*, 621−630.
(11) Chaskar, A.; Chen, H.-F.; Wong, K.-T. Bipolar Host Materials: A Chemical Approach for Highly Efficient Electrophosphorescent Devices. *Adv. Mater.* **2011**, *23*, 3876−3895.
(12) Jeon, S. O.; Lee, J. Y. *J. Mater. Chem.* **2012**, *22*, 4233−4243.
(13) Tao, Y.; Wang, Q.; Yang, C.; Wang, Q.; Zhang, Z.; Zou, T.; Qin, J.; Ma, D. A Simple Carbazole/Oxadiazole Hybrid Molecule: An Excellent Bipolar Host for Green and Red Phosphorescent OLEDs. *Angew. Chem., Int. Ed.* **2008**, *47*, 8104−8107.
(14) Fan, C.; Zhao, F.; Gan, P.; Yang, S.; Liu, T.; Zhong, C.; Ma, D.; Qin, J.; Yang, C. Simple Bipolar Molecules Constructed from Biphenyl Moieties as Host Materials for Deep-Blue Phosphorescent Organic Light-Emitting Diodes. *Chem.—Eur. J.* **2012**, *18*, 5510−5514.
(15) Gong, S.; Zhao, Y.; Yang, C.; Zhong, C.; Qin, J.; Ma, D. Tuning the Photophysical Properties and Energy Levels by Linking Spacer and Topology between the Benzimidazole and Carbazole Units: Bipolar Host for Highly Efficient Phosphorescent OLEDs. *J. Phys. Chem. C* **2010**, *114*, 5193−5198.
(16) Duan, L.; Qiao, J.; Sun, Y.; Qiu, Y. Strategies to Design Bipolar Small Molecules for OLEDs: Donor-Acceptor Structure and Non-Donor-Acceptor Structure. *Adv. Mater.* **2011**, *23*, 1137−1144.
(17) Wen, S.-W.; Lee, M.-T.; Chen, C. H. Recent Development of Blue Fluorescent OLED Materials and Devices. *J. Disp. Technol.* **2005**, *1*, 90−99.
(18) Ho, M.-H.; Wu, Y.-S.; Wen, S.-W.; Lee, M.-T.; Chen, T.-M.; Chen, C. H.; Kwok, K.-C.; So, S.-K.; Yeung, K.-T.; Cheng, Y.-K.; Gao, Z.-Q. Highly Efficient Deep Blue Organic Electroluminescent Device Based on 1-Methyl-9,10-di(1-naphthyl)anthracene. *Appl. Phys. Lett.* **2006**, *89*, 252903-1−252903-3.
(19) Liu, T.-H.; Wu, Y.-S.; Lee, M.-T.; Chen, H.-H.; Liao, C.-H.; Chen, C. H. Highly Efficient Yellow and White Organic Electroluminescent Devices Doped with 2,8-Di(t-butyl)-5,11-di[4-(t-butyl)-phenyl]-6,12-diphenylnaphthacene. *Appl. Phys. Lett.* **2004**, *85*, 4304−4306.

(20) Lee, Y. G.; Lee, H.-N.; Kang, S. K.; Oh, T. S.; Lee, S.; Koh, K. H. Fabrication of Highly Efficient and Stable Doped Red Organic Light-Emitting Device Using 2-Methyl-9,10-di(2-naphthyl)anthracene and Tris(8-hydroxyquinolinato)aluminum as Cohost Materials. *Appl. Phys. Lett.* **2006**, *89*, 183515−1−183515−3.
(21) Lee, Y. G.; Kang, S. K.; Oh, T. S.; Lee, H.-N.; Lee, S.; Koh, K. H. Comparison of Two Cohost Systems for Doped Red Organic Light-Emitting Devices in an Effort to Improve the Efficiency and the Lifetime. *Org. Electron.* **2008**, *9*, 339−346.
(22) Ho, M.-H.; Liu, M.-Y.; Lin, K.-H.; Chen, C. H.; Tang, C. W. Efficient Single-Layer Small Molecule Blue OLEDs Based on a Multifunctional Bipolar Transport Material. *SID Symp. Dig. Tech. Pap.* **2010**, *41*, 552−555.
(23) Cai, X.; Padmaperuma, A. B.; Sapochak, L. S.; Vecchi, P. A.; Burrows, P. E. Electron and Hole Transport in a Wide Bandgap Organic Phosphine Oxide for Blue Electrophosphorescence. *Appl. Phys. Lett.* **2008**, *92*, 083308−1−083308−3.
(24) Chu, M.-T.; Lee, M.-T.; Chen, C. H.; Tseng, M.-R. Improving the Performance of Blue Phosphorescent Organic Light-Emitting Devices Using a Composite Emitter. *Org. Electron.* **2009**, *10*, 1158−1162.
(25) Jeong, S. H.; Lee, J. Y. Dibenzothiophene Derivatives as Host Materials for High Efficiency in Deep Blue Phosphorescent Organic Light Emitting Diodes. *J. Mater. Chem.* **2011**, *21*, 14604−14609.
(26) Ren, Z.; Zhang, R.; Ma, Y.; Wang, F.; Yan, S. Synthesis of Ring-Structured Polysiloxane as Host Materials for Blue Phosphorescent Device. *J. Mater. Chem.* **2011**, *21*, 7777−7781.
(27) Bin, J.-K.; Yang, J. H.; Hong, J.-I. New Sulfur-Containing Host Materials for Blue Phosphorescent Organic Light-Emitting Diodes. *J. Mater. Chem.* **2012**, *22*, 21720−21726.
(28) Han, C.; Zhang, Z.; Xu, H.; Yue, S.; Li, J.; Yan, P.; Deng, Z.; Zhao, Y.; Yan, P.; Liu, S. Short-Axis Substitution Approach Selectively Optimizes Electrical Properties of Dibenzothiophene-Based Phosphine Oxide Hosts. *J. Am. Chem. Soc.* **2012**, *134*, 19179−19188.
(29) Dong, S.-C.; Gao, C.-H.; Yuan, X.-D.; Cui, L.-S.; Jiang, Z.-Q.; Lee, S.-T.; Liao, L.-S. Novel Dibenzothiophene Based Host Materials Incorporating Spirobifluorene for High-Efficiency White Phosphorescent Organic Light-Emitting Diodes. *Org. Electron.* **2013**, *14*, 902−908.
(30) Dong, S.-C.; Liu, Y.; Li, Q.; Cui, L.-S.; Chen, H.; Jiang, Z.-Q.; Liao, L.-S. Spiro-Annulated Tiarylamine-Based Hosts Incorporating Dibenzothiophene for Highly Efficient Single-Emitting Layer White Phosphorescent Organic Light-Emitting diodes. *J. Mater. Chem. C* **2013**, *1*, 6575−6584.
(31) Togashi, K.; Yasuda, T.; Adachi, C. Triphenylene-Based Host Materials for Low-voltage, Highly Efficient Red Phosphorescent Organic Light-Emitting Diodes. *Chem. Lett.* **2013**, *42*, 383−385.
(32) Lin, W.-C.; Huang, W.-C.; Huang, M.-H.; Fan, C.-C.; Lin, H.-W.; Chen, L.-Y.; Liu, Y.-W.; Lin, J.-S.; Chao, T.-C.; Tseng, M.-R. A Bipolar Host Containing Carbazole/Dibenzothiophene for Efficient Solution-Processed Blue and White Phosphorescent OLEDs. *J. Mater. Chem. C* **2013**, *1*, 6835−6841.
(33) Yang, W.; Hou, Q.; Liu, C.; Niu, Y.; Huang, J.; Yang, R.; Cao, Y. Improvement of Color Purity in Blue-Emitting Polyfluorene by Copolymerization with Dibenzothiophene. *J. Mater. Chem.* **2003**, *13*, 1351−1355.
(34) Huang, T.-H.; Lin, J. T.; Chen, L.-Y.; Lin, Y.-T.; Wu, C.-C. Dipolar Dibenzothiophene S,S-Dioxide Derivatives Containing Diarylamine: Materials for Single-Layer Organic Light-Emitting Devices. *Adv. Mater.* **2006**, *18*, 602−606.
(35) Wang, L.; Wu, Z.-Y.; Wong, W.-Y.; Cheah, K.-W.; Huang, H.; Chen, C. H. New Blue Host Materials Based on Anthracene-Containing Dibenzothiophene. *Org. Electron.* **2011**, *12*, 595−601.
(36) Qiao, Y.; Wei, Z.; Risko, C.; Li, H.; Bredas, J.-L.; Xu, W.; Zhu, D. Synthesis, Experimental and Theoretical Characterization, and Field-Effect Transistor Properties of a New Class of Dibenzothiophene Derivatives: From Linear to Cyclic Architectures. *J. Mater. Chem.* **2012**, *22*, 1313−1325.
(37) Su, S.-J.; Cai, C.; Kido, J. RGB Phosphorescent Organic Light-Emitting Diodes by Using Host Materials with Heterocyclic Cores: Effect of Nitrogen Atom Orientations. *Chem. Mater.* **2011**, *23*, 274−284.
(38) Gong, S.; He, X.; Chen, Y.; Jiang, Z.; Zhong, C.; Ma, D.; Qin, J.; Yang, C. Simple CBP Isomers with High Triplet Energies for Highly Efficient Blue Electrophosphorescence. *J. Mater. Chem.* **2012**, *22*, 2894−2899.
(39) Martin, R. L. Natural Transition Orbitals. *J. Chem. Phys.* **2003**, *118*, 4775−4777.
(40) D'Andrade, B. W.; Datta, S.; Forrest, S. R.; Djurovich, P.; Polikarpov, E.; Thompson, M. E. Relationship Between the Ionization and Oxidation Potentials of Molecular Organic Semiconductors. *Org. Electron.* **2005**, *6*, 11−20.
(41) Djurovich, P. I.; Mayo, E. I.; Forrest, S. R.; Thompson, M. E. Measurement of the Lowest Unoccupied Molecular Orbital Energies of Molecular Organic Semiconductors. *Org. Electron.* **2009**, *10*, 515−520.
(42) Salman, S.; Kim, D.; Coropceanu, V.; Brédas, J.-L. Theoretical Investigation of Triscarbazole Derivatives As Host Materials for Blue Electrophosphorescence: Effects of Topology. *Chem. Mater.* **2011**, *23*, 5223−5230.
(43) Lu, T.; Chen, F. Multiwfn: A Multifunctional Wavefunction Analyzer. *J. Comput. Chem.* **2012**, *33*, 580−592.
(44) Jou, J.-H.; Wu, M.-H.; Shen, S.-M.; Wang, H.-C.; Chen, S.-Z.; Chen, S.-H.; Lin, C.-R.; Hsieh, Y.-L. Sunlight-Style Color-Temperature Tunable Organic Light-Emitting Diode. *Appl. Phys. Lett.* **2009**, *95*, 013307−1−013307−3.
(45) Jou, J.-H.; Chen, P.-W.; Chen, Y.-L.; Jou, Y.-C.; Tseng, J.-R.; Wu, R.-Z.; Hsieh, C.-Y.; Hsieh, Y.-C.; Joers, P.; Chen, S.-H.; Wang, Y.-S.; Tung, F.-C.; Chen, C.-C.; Wang, C.-C. OLEDs with Chromaticity Tunable Between Dusk-hue and Candle-light. *Org. Electron.* **2013**, *14*, 47−54.
(46) Liaptsis, G.; Meerholz, K. Crosslinkable TAPC-Based Hole-Transport Materials for Solution-Processed Organic Light-Emitting Diodes with Reduced Efficiency Roll-Off. *Adv. Funct. Mater.* **2013**, *23*, 359−365.
(47) Krummacher, B.; Mathai, M. K.; Choong, V.-E.; Choulis, S. A.; So, F.; Winnacker, A. Influence of Charge Balance and Microcavity Effects on Resultant Efficiency of Organic-Light Emitting Devices. *Org. Electron.* **2006**, *7*, 313−318.
(48) Wu, Z.; Wang, L.; Lei, G.; Qiu, Y. Investigation of the Spectra of Phosphorescent Organic Light-Emitting Devices in Relation to Emission Zone. *J. Appl. Phys.* **2005**, *97*, 103105−1−103105−4.